Energy Efficiency Maximization in Cooperative Hybrid VLC/RF Networks with NOMA

Konstantinos G. Rallis*, Vasilis K. Papanikolaou*, Panagiotis D. Diamantoulakis*,
Mohammad-Ali Khalighi†, George K. Karagiannidis*
*Department of Electrical and Computer Engineering, Aristotle University of Thessaloniki, GR-54124 Thessaloniki, Greece
†Aix-Marseille University, CNRS, Centrale Marseille, Institut Fresnel, Marseille, France
e-mails: konralgeo@ece.auth.gr, vpapanikk@auth.gr, padiaman@ieee.org, Ali.Khalighi@fresnel.fr, geokarag@auth.gr

2021 17th International Symposium on Wireless Communication Systems (ISWCS) | 978-1-7281-7432-7/21/$31.00 ©2021 IEEE | DOI: 10.1109/ISWCS49558.2021.9562202

***Abstract*—In this paper, a cooperative hybrid visible light communications (VLC)/radio frequency (RF) network that employs non-orthogonal multiple access (NOMA) is investigated. More specifically, the resource allocation and the operating mode of the system is optimized to maximize a weighted energy efficiency metric, taking into accounts the particularities of the hybrid network. The resulting optimization problem is efficiently tackled with the use of Dinkelbach's algorithm and difference of convex programming. Using this solution, a deep neural network (DNN) is trained to find the operation mode and alleviate the computational cost of the overall problem leading to a close solution to the optimal. Finally, the effectiveness of the proposed setup is presented via Monte Carlo simulation results.**

I. Introduction

A major limitation of conventional radio frequency (RF) communications has been the ever increasing crowding of the RF spectrum, due to the growing number of connected devices and amount of data they require. To address these concerns, academia and industry have shifted their attention to emerging technologies, such as optical wireless communications (OWC), that utilize a different region of the electromagnetic spectrum, meaning they would be able to serve a plethora of devices with no interference to the RF network [1]. More specifically, optical wireless access indoors has been mostly facilitated via visible light communications (VLC) technology through the use of light emitting diodes (LED) bulbs, which can offer high data rate communications at a low cost through the illumination infrastructure. VLC also offers high inherent physical layer security and a high frequency reuse factor since light is blocked by opaque structures such as walls. Due to these advantages, VLC has been recognized as a potential candidate technology for the 5G Public-Private-Partnership (PPP) project, while there are global efforts on VLC standardization such as IEEE P802.11bb. On the other hand, line-of-sight (LoS) can easily be blocked by the movement or rotation of the receiver and also VLC is in general dependent on the room illumination levels. The above reasons have led to the proposed heterogeneous networking of RF and VLC networks, in order to maintain coverage via RF while boasting higher data rates through VLC. Hybrid VLC/RF networks have been extensively studied during the recent years [2] as a way to capitalize on the unused electromagnetic (EM) spectrum for wireless access.

Apart from the growing interest in previously unexploited regions of the EM spectrum, the efficient use of the available bandwidth is of paramount importance. To this end, non-orthogonal multiple access (NOMA) has attracted significant attention from the research community due to its increased spectral efficiency. NOMA with VLC has been examined in [3]–[5] and it was also shown experimentally in [6], while hybrid VLC/RF networks with NOMA were studied in [7]–[10]. Cooperative hybrid VLC/RF networks with NOMA were examined in terms of outage probability in [8]. In that paper, a cross-band selection diversity combining scheme is proposed to improve the system's performance.

Moreover, the increasing number of access points (APs) is concerning given the resulting energy consumption. However, VLC APs which are usually already on for illumination coverage, can offer wireless access with minimal additional energy consumption. As such, VLC has been recognized as a promising indoor wireless network to reduce the energy requirements and improve energy efficiency. In this regard, in [11], the authors examined the resource allocation in a hybrid VLC/RF network to maximize the energy efficiency of the system, while in [12], the authors minimized the energy consumption of a hybrid VLC/RF network while satisfying the users' quality of service (QoS) requirements. Additionally, in [13] the authors designed a hybrid VLC/RF network with a power line communications (PLC) backhaul and maximize the energy efficiency via optimizing the power allocation of the VLC/RF network and the backhaul flow of the PLC network. Moreover, in [14], hybrid VLC/RF networks with a decode and forward relaying setup were investigated in terms of physical layer security. More recently, in [9], [10], the authors investigated the power allocation and user pairing in a cooperative setup like the one [8], with the aim to maximize the sum rate while satisfying QoS constraints of the users.

Motivated by the former results, in this paper, we investigate a cooperative hybrid VLC/RF network to maximize a weighted energy efficiency metric. The proposed metric takes into account the particularities imposed by the illumination function of the VLC APs. The cooperative network makes use of NOMA to serve its users via the VLC AP, while an RF link is present between the users for possible cooperation. The operation mode of the network is chosen to optimize energy efficiency and the resulting optimization problem is

tackled with the use of a Dinkelbach based algorithm and difference of convex programming. Finally, in order to reduce the computational complexity of the proposed solution, a deep neural network (DNN) is trained to chose the operation mode of the network given the users' channel state information and QoS constraints. After training, the DNN can offer close to optimal performance at a fraction of the cost.

II. System Model

We consider an indoor downlink system, consisting of one VLC AP and two types of users, namely a *near* user, denoted as U_1, and a *far* user, denoted as U_2. The users' locations are uniformly distributed in a cyclic disk with radius R_0 and an annular area bounded by radii R_0 and R_v, respectively. Polar coordinates (r_i, θ_i) are utilized to describe the exact position of user i from the center. Moreover, the VLC AP is placed on the ceiling with a vertical distance L from the ground plane. Both U_1 and U_2 are assumed to belong in the coverage area of the VLC AP. The VLC AP utilized NOMA for downlink transmission to U_1 and U_2 simultaneously, while U_1 can also act as a full-duplex (FD) decode-and-forward (DF) RF relay to assist the far user U_2.

A. VLC Transmission

VLC transmission employs intensity modulation-direct detection (IM-DD) NOMA. The non-negative optical transmitted superposed signal is defined as $x = \sqrt{P_1}x_1 + \sqrt{P_2}x_2$, with P_1 and P_2 being the transmitted power allocated for user U_1 and U_2, respectively. To maintain illumination levels as well as to guarantee safety and hardware constraints, the maximum transmitted optical power is limited to $P_{\max}^{\text{VLC}}$. Therefore, it holds that

$$P_1 + P_2 \leq P_{\max}^{\text{VLC}}. \tag{1}$$

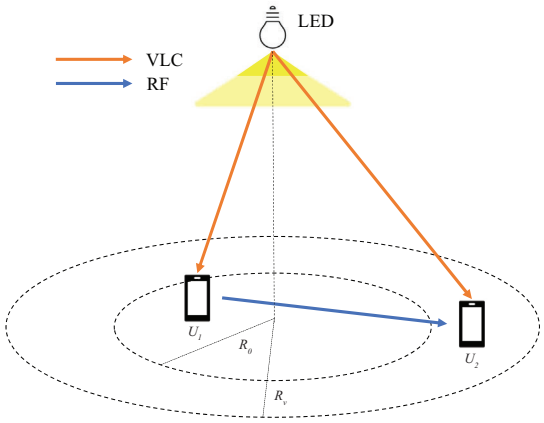

Fig. 1. System Model.

Accordingly, the received message at user U_i can be expressed as

$$y_i = \eta h_i x + n_i, \tag{2}$$

where η is the photo-detector responsivity in A/W, h_i is the VLC channel gain between the VLC AP and U_i, and n_i is the additive white Gaussian noise (AWGN) at U_i. Assuming LoS, the VLC channel gain is given by [15], [16]

$$h_i = \frac{m+1}{2\pi d_i^2} A_r \cos^m(\phi_i) T(\psi_i) g(\psi_i) cos(\psi_i), \tag{3}$$

where A_r is the detector area of the photodiode at user U_i, ϕ_i and ψ_i denote the irradiance and the incidence angles of U_i, respectively, while m is the Lambertian emission order, which is obtained as

$$m = -\ln 2 / \ln(\cos(\Phi_{1/2})), \tag{4}$$

where $\Phi_{1/2}$ is the transmitter semi-angle at half-power. On top of that, the distance d_i is expressed as $d_i = \sqrt{r_i^2 + L^2}$ regarding the polar coordinates of user U_i and the ceiling height L. Moreover, $T(\psi_i)$ and $g(\psi_i)$ denote the gains of the optical filter and the optical concentrator, respectively, with the latter being expressed as

$$g(\psi_i) = \begin{cases} \frac{n^2}{\sin^2 \Psi_{\text{FOV}}}, & 0 \leq \psi_i \leq \Psi_{\text{FOV}} \\ 0, & \psi_i > \Psi_{\text{FOV}}, \end{cases} \tag{5}$$

where Ψ_{FOV} denotes the field-of-view (FOV) of the transmitter and n is the refractive index.

Without loss of generality, we assume that the optical detector of each user is pointing upwards so that it holds that $\phi_i \approx \psi_i$. Then, taking into account the polar coordinates system, the channel gain from the VLC AP to the VLC user is given by

$$h_i = \frac{C(m+1)L^{(m+1)}}{(r_i^2 + L^2)^{\frac{m+3}{2}}}, \tag{6}$$

where $C = \frac{A_r T(\psi_i) g(\psi_i)}{2\pi d_i^2}$.

According to the power domain NOMA principle, the weak user U_2 decodes its own message with an achievable rate $R_{2,V}$ by treating U_1's message as interference. At the strong user's detector, i.e., at U_1, the message meant for U_2 is first decoded to be removed via successive interference cancellation (SIC). The rate at which U_1 can decode the message of U_2 is $R_{2\to1,V}$. Following this, U_1 decodes its own message without interference with an achievable rate equal to $R_{1,V}$. Due to the intensity modulation-direct detection (IM/DD) utilized by the VLC system, the common Shannon formula cannot be used to evaluate the capacity since there are a number of additional constraints for the transmitted signal, including the non-negativity limitation of the input signal that modulates the optical intensity of the emitted light and the constraint on the total optical transmit power transmitted. Instead, by utilizing a lower bound of the corresponding capacity region, the achievable rates for each user can be described as [17]

$$R_{2\to1,V} = B_v \log_2 \left(1 + \frac{(\eta h_1 P_2)^2}{((\eta h_1 P_1)^2 + 9\sigma^2)(1+\epsilon_\mu)^2}\right) - \epsilon_\phi, \tag{7}$$

$$R_{1,V} = B_v \log_2 \left(1 + \frac{(\eta h_1 P_1)^2}{9\sigma^2(1+\epsilon_\mu)^2}\right) - \epsilon_\phi, \tag{8}$$

$$R_{2,V} = B_v \log_2 \left(1 + \frac{(\eta h_2 P_2)^2}{((\eta h_2 P_1)^2 + 9\sigma^2)(1+\epsilon_\mu)^2}\right) - \epsilon_\phi, \tag{9}$$

where B_v is the bandwidth of the VLC network, σ^2 is the noise variance and $\epsilon_\phi = 0.016$, $\epsilon_\mu = 0.0015$.

B. RF Transmission

During RF transmission, the baseband equivalent received signal at the terminal of user U_2 is expressed as follows

$$y_R = \sqrt{P_{\mathrm{RF}}} x_t h_{\mathrm{RF}} + n_R, \tag{10}$$

where n_R is the AWGN noise at the RF receiver with variance σ_R^2, $h_{\mathrm{RF}} \sim \text{Rician}(K_r, d_{\mathrm{RF}}^{-\zeta})$ is the Rician RF channel. Without loss of generality, Rician fading is assumed since a strong LoS component is almost certainly present between the two indoor users as they are described in this scenario. Moreover P_{RF} denotes the available power for retransmission at U_1 and ζ is the path-loss exponent. Given the topology of the scenario and by utilizing the polar coordinates of U_1 and U_2, d_{RF}, which is the Euclidean distance between the two users, can be calculated by

$$d_{\mathrm{RF}} = \sqrt{r_1^2 + r_2^2 - 2 r_1 r_2 \cos(\theta_2 - \theta_1)} \tag{11}$$

Taking into account the path-loss formula $L_{\mathrm{RF}}^{\mathrm{dB}} = L_{d_0} + 10\zeta \log_{10}(\frac{d_R}{d_0})$, $L_{\mathrm{RF}} = 10^{\frac{L_{\mathrm{RF}}^{\mathrm{dB}}}{10}}$, where $L_{d_0} = 68dB$ and $d_0 = 1$ m, the achievable data rate from U_1 to U_2 via the RF link, according to Shannon capacity, is given by:

$$R_{2,R} = B_R \log_2 \left(1 + \frac{L_{\mathrm{RF}} |h_{\mathrm{RF}}|^2 P_{\mathrm{RF}}}{\sigma_R^2}\right), \tag{12}$$

where B_R denotes the bandwidth of the RF system.

III. Energy Efficiency Optimization

In this section, the resource allocation of the hybrid VLC/RF network is investigated in order to maximize an energy efficient metric, while the users of the network fulfill their QoS requirements. Energy efficiency is defined as the ratio of achievable data rate per consumed power. In order to better capture the particularities of the heterogeneity of this type of network, such as the dependency of VLC transmission power to the illumination levels, a weighted energy efficiency metric is examined. More specifically, a weight α with $0 \leq \alpha \leq 1$ is used to tune the users' throughput, while a weight β, $0 \leq \beta \leq 1$, adjusting the focus of the metric on the consumed power of each network. As such, the weighted energy efficiency metric that is studied in this paper is expressed as

$$\mathrm{EE} = \frac{\alpha R_1 + (1-\alpha) R_2}{\beta P_{\mathrm{VLC}} + (1-\beta) P_{\mathrm{RF}}}, \tag{13}$$

where $P_{\mathrm{VLC}} = P_1 + P_2$ and R_2 is the achievable data rate of the second user, depending on the mode q of the cooperative network, i.e.,

$$R_2 = q R_{2,V} + (1-q) R_{2,R}, q \in \{0, 1\}, \tag{14}$$

where $q = 1$ is the pure VLC mode, while $q = 0$ is the cooperative RF mode.

Considering the achievable data rates of each user, their QoS constraints, and the required power for consumption, the following optimization problem to maximize energy efficiency is defined

$$\begin{aligned} \max_{q, P_1, P_2, P_{\mathrm{RF}}} \quad & \tfrac{\alpha R_1 + (1-\alpha) R_2}{\beta P_{\mathrm{VLC}} + (1-\beta) P_{\mathrm{RF}}} \\ \text{s.t.} \quad & \mathrm{C}_1 : R_{1,V} \geq R_1^{\mathrm{thr}}, \\ & \mathrm{C}_2 : R_2 \geq R_2^{\mathrm{thr}}, \\ & \mathrm{C}_3 : R_{2\to 1,V} \geq R_2^{\mathrm{thr}}, \\ & \mathrm{C}_4 : \textstyle\sum_{i \in \mathrm{VLC}} P_i^{\mathrm{VLC}} \leq P_{\max}^{\mathrm{VLC}}, \\ & \mathrm{C}_5 : P_2^{\mathrm{RF}} \leq P_{\max}^{\mathrm{RF}}, \end{aligned} \tag{15}$$

where C_1 and C_2 are the QoS requirements of the users U_1 and U_2, respectively. U_2 can achieve their requirement with either the VLC network or through the cooperative strategy. Since NOMA is utilized in this scenario, U_1 is required to be able to decode U_2's message for two reasons; first, it is required for U_1 to perform SIC and decode their own message, and second in order to be able to transmit via RF the message to user U_2. Therefore, constraint C_3 ensures that the rate at which U_1 decodes U_2's message fulfills their QoS constraint. Finally, as mentioned in the previous section, the power consumption levels of the AP and U_1 are bounded by illumination and hardware constraints leading to C_4 and C_5.

The optimization problem in (15) is a mixed integer nonlinear optimization problem. In order to solve this problem we perform a full search on the integer value q, since it can only take values of either zero or one. Following that, problem (15) reduces to a nonlinear problem. However, it is noted that the problem is non-convex, mainly due to the fractional objective function and constraints C_1, C_2, and C_3, which contain the logarithms with squared power terms. In order to efficiently solve this problem in polynomial time, we need to transform it into an equivalent convex than can be efficiently solved by efficient fractional programming techniques, including convex optimization tools. To do so, first, we introduce two auxiliary variables r_1 and r_2, such that

$$R_1^{\mathrm{thr}} \leq r_1 \leq R_{1,V} \text{ and } R_1^{\mathrm{thr}} \leq r_2 \leq R_2, \tag{16}$$

which change the constraints and introduce C_6 and C_7. As such, the problem (15) is formulated as:

$$\begin{aligned} \max_{q, r_1, r_2, P_1, P_2, P_{\mathrm{RF}}} \quad & \tfrac{\alpha r_1 + (1-\alpha) r_2}{\beta P_{\mathrm{VLC}} + (1-\beta) P_{\mathrm{RF}}} \\ \text{s.t.} \quad & \mathrm{C}_1 : R_{2\to 1,V} \geq R_2^{\mathrm{thr}}, \\ & \mathrm{C}_2 : \textstyle\sum_{i \in \mathrm{VLC}} P_i^{\mathrm{VLC}} \leq P_{\max}^{\mathrm{VLC}} \\ & \mathrm{C}_3 : P_2^{\mathrm{RF}} \leq P_{\max}^{\mathrm{RF}}, \\ & \mathrm{C}_4 : r_1 \leq R_{1,V}, \\ & \mathrm{C}_5 : r_2 \leq R_2, \\ & \mathrm{C}_6 : r_1 \geq R_1^{\mathrm{thr}}, \\ & \mathrm{C}_7 : r_2 \geq R_2^{\mathrm{thr}}. \end{aligned} \tag{17}$$

The objective function's form makes problem (17) a fractional programming problem. To solve this, Dinkelbach's algorithm is applied [18]. Dinkelbach's algorithm is an iterative process that solves an equivalent parametric problem given as the difference between the numerator and the denominator

multiplied by a parameter. As such, we set $F = \alpha r_1 + (1-\alpha) r_2$ and $G = \beta P_{\mathrm{VLC}} + (1-\beta) P_{\mathrm{RF}}$. To maximize an objective function with Dinkelbach's algorithm, F should be concave and G should be convex. In this case, both functions are affine, so Dinkelbach's algorithm can be utilized. The fractional problem $\max\{U(z) = F(z)/G(z)\}$ can then be related to

$$H(u) = \max\{F(z) - uG(z)\},\ u \in \mathbb{R}, \tag{18}$$

with $z = [r_1, r_2, P_1, P_2, P_{\mathrm{RF}}]$. Following that, our aim is to find an optimal solution z_i of $H(u_i)$ in each iteration i of the algorithm.

$\hat{H}$ is continuous, convex and strictly decreasing in $\mathbb{R}$. It is assumed that $\tilde{z}^+$ is optimal, if and only if it is optimal for $H(u^+)$, where u^+ is the only zero of H. The Dinkelbach's Algorithm applied is explained in Algorithm 1.

Algorithm 1: Dinkelbach's Algorithm

Initialization: Set the initial point $u_0 < u^+$, for example $u_0 = U(z_0) > 0$ for some z_0. Also set iteration index $i = 0$ and the convergence accuracy ϵ;
while $H(u_i) > \epsilon$ *(for some ϵ given)* **do**
  Calculate an optimal solution z_i of $H(u_i)$ s.t. (17).C_1 − (17).C_7 ; Let $u_{i+1} = U(z_i)$;
  $i \leftarrow i + 1$;
end
Result: optimal u^+,z^+

In Algorithm 1, constraints (17).C_1 − (17).C_7 still hold. However the problem remains non-convex and in order to be able to find a tractable solution in polynomial time, it is of essence to transform the problem to an equivalent convex one. We start by employing the geometric programming transformation, i.e.,

$$\begin{aligned} &r_1 = e^{\tilde{r}_1}, && r_2 = e^{\tilde{r}_2}, \\ &P_1 = e^{p_1}, && P_2 = e^{p_2}, \quad P_{\mathrm{RF}} = e^{p_{\mathrm{RF}}}, \end{aligned} \tag{19}$$

leading to $\tilde{z} = [\tilde{r}_1, \tilde{r}_2, \tilde{p}_1, \tilde{p}_2, \tilde{p}_{\mathrm{RF}}]$ and $e^{p_1} + e^{p_2} = e^{p_{\mathrm{VLC}}}$. After the transformation, the problem is expressed as follows

$$\begin{aligned} \max_{q,\tilde{z}} \quad & \alpha e^{\tilde{r}_1} + (1-\alpha) e^{\tilde{r}_2} - u\left(\beta e^{p_{\mathrm{VLC}}} + (1-\beta) e^{p_{\mathrm{RF}}}\right) \\ \text{s.t.} \quad & \mathrm{C}_1 : \log\left(e^{2p_1} + \tfrac{9\sigma^2}{(\eta h_1)^2}\right) - 2p_2 \\ & + \log\left((1+\epsilon_\mu)^2 (2^{\frac{R_2^{\mathrm{thr}} + \epsilon_\phi}{B_v}} - 1)\right) \le 0 \\ & \mathrm{C}_2 : e^{p_1} + e^{p_2} \le P_{\max}^{\mathrm{VLC}} \\ & \mathrm{C}_3 : p_{\mathrm{RF}} \le \log(P_{\max}^{\mathrm{RF}}) \\ & \mathrm{C}_4 : \log\left(2^{\frac{e^{\tilde{r}_1} + \epsilon_\phi}{B_v}} - 1\right) - 2p_1 - \log\left(\tfrac{(\eta h_1)^2}{9\sigma^2 (1+\epsilon_\mu)^2}\right) \le 0 \\ & \mathrm{C}_5^{(q=1)} : \log\left(2^{\frac{e^{\tilde{r}_2} + \epsilon_\phi}{B_v}} - 1\right) + \log\left(e^{2p_1} + \tfrac{9\sigma^2}{(\eta h_2)^2}\right) \\ & -2p_2 + \log((1+\epsilon_\mu)^2) \le 0 \\ & \mathrm{C}_5^{(q=0)} : \log\left(2^{\frac{e^{\tilde{r}_2}}{B_R}} - 1\right) - p_{\mathrm{RF}} - \log\left(\tfrac{L_{\mathrm{RF}} h_{\mathrm{RF}}}{\sigma_R}\right) \le 0 \\ & \mathrm{C}_6 : \tilde{r}_1 \ge \log(R_1^{\mathrm{thr}}) \\ & \mathrm{C}_7 : \tilde{r}_2 \ge \log(R_2^{\mathrm{thr}}). \end{aligned} \tag{20}$$

Constraints C_2, C_3, C_6, and C_7 are easily shown to be convex. More specifically, the first term of C_1 and the second term of $\mathrm{C}_5^{(q=1)}$ are convex as log-sum-exp terms. The remaining of terms that are needed to be convex are in the form of $f(t) = \log\left(C_0 2^{e^t/C_1} - 1\right)$. The second derivative of $f(t)$ with respect to t can be written as $\frac{d^2 f}{dt^2} = \frac{2^q C_0 q (C_0 2^q - 1 - q\log(2))}{(C_0 2^q - 1)^2}$, where $q = \exp(t)/C_1$ and $C_0, C_1 > 0$. Considering $\xi = C_0 2^q - q\log(2) - 1$ is an increasing function with respect to q and when $q \to 0$, $\xi \to 0$, it is shown that $\frac{d^2 f}{dt^2} \ge 0$. Following that, it is proven that $f(t)$ is convex with respect to t.

We define the objective function of (20) as $\Xi(\tilde{z}, u) = \alpha e^{\tilde{r}_1} + (1-\alpha) e^{\tilde{r}_2} - u\left(\beta e^{p_{\mathrm{VLC}}} + (1-\beta) e^{p_{\mathrm{RF}}}\right) = \Phi(\tilde{z}) - u\Theta(\tilde{z})$. We observe that Ξ is convex with respect to u, but it is a difference of convex (DC) function with respect to $\tilde{z}$. Therefore, to calculate the optimal solution of (20) to plug into Algorithm 1, we have to apply a DC Algorithm (DCA) [19]. DCA is an iterative algorithm based on local optimality conditions and duality. It is noted that we choose to minimize the $-\Xi(\tilde{z}, u_i)$ problem which is equivalent to maximize the $\Xi(\tilde{z}, u_i)$ one. The idea of DCA is that at each iteration, the second component in the primal DC problem is replaced by its affine minorization in order to generate the convex problem

$$\begin{aligned} \min_{\tilde{z}} \quad & \hat{\Xi}(\tilde{z}, u) \\ \text{s.t.} \quad & (20).\mathrm{C}_1 - (20).\mathrm{C}_7, \end{aligned} \tag{21}$$

where $\hat{\Xi}(\tilde{z}, u) = u\Theta(\tilde{z}) - (\Phi(\tilde{z}_k) + \nabla\Phi(\tilde{z}_k)^T(\tilde{z} - \tilde{z}_k))$.

The DCA scheme is described in Algorithm 2.

Algorithm 2: DCA

Initialization: Choose an initial point $\tilde{z}_0, \tilde{z}_{-1} \in \mathbb{R}^N$ and Let $k = 0$;
Set iteration index $i = 0$ and the convergence accuracy ϵ;
while $\hat{\Xi}(\tilde{z}_k, u_i) - \hat{\Xi}(\tilde{z}_{k-1}, u_i) > \epsilon$ **do**
  Compute $\nabla\Phi(\tilde{z}_k)$;
  Calculate an optimal solution $\tilde{z}_{k+1}$ for convex problem (21);
  $k \leftarrow k + 1$;
end
Result: optimal $\tilde{z}^+$

The resulting convex optimization problem can be efficiently solved with convex optimization methods in polynomial time, such as the interior-point method [20]. Following that, optimal $\tilde{z}$ is transformed to z through (19) and it is plugged into Algorithm 1, in order to find the optimal u. At the end of this iterative process the optimal resource allocation is obtained. The operation mode q is selected from the solution that maximizes the total energy efficiency.

IV. Multi-layer Perceptron for Mode Classification

In order to reduce the complexity of obtaining the optimum as was described in the previous section, we design

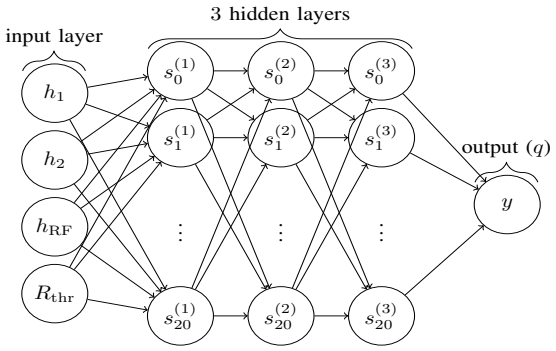

Fig. 2. Network graph of the proposed MLP

a deep neural network (DNN) to perform classification in order to determine the operation mode of the network [21]. More specifically, our DNN model is a multi-layer perceptron (MLP), which is a feedforward network making it much easier to train. To train the MLP, training sets are generated via the optimal algorithm described in section III.

The training data are denoted as $(\mathbf{x}, y)$, where the input x refers to the channel vector $\mathbf{h} = [h_1, h_2, h_{\mathrm{RF}}]$ and the QoS requirements of the users $\mathbf{R}_{\mathrm{thr}} = R_1^{\mathrm{thr}} = R_2^{\mathrm{thr}}$. So $\mathbf{x} = [\mathbf{h}, \mathbf{R}_{\mathrm{thr}}]$. The output y of the MLP is continuous in $[0, 1]$ an as such it cannot directly set the value of q. Therefore, for any fractional value $0.5 \leq y \leq 1$, we set $q = 1$, otherwise if $0 \leq y < 0.5$, the value $q = 0$ is chosen. Apart from the input and output layers, the MLP consists of a 3 hidden layers. Each hidden layer consists of a total of 20 nodes. The activation function for the three hidden layers is ReLU, while for the output layer the sigmoid function was used. In order to increase the accuracy of the MLP, a pre-processing of the data took place through a min-max scaler pre-processor, which translates the input values to a range of [0,1] given their minimum and maximum values in the set.

V. Numerical Results and Discussion

In this section, Monte Carlo simulation results are presented for the proposed system for 10^4 iterations. The simulation parameters can be found in Table I. More specifically, in Figs 3 and 4, the effect of the weighting factors α and β on the energy efficiency versus the threshold rates of the users can be observed. Without loss of generality, the two users are presented with identical QoS constraints in these results.

TABLE I
Simulation Parameters

Parameter	Value	Parameter	Value
B_v	40 MHz	σ^2	4×10^{-22}
B_R	10 MHz	σ_R^2	$4.002 \times 10^{-21} B_R$
R_0	1.5 m	$T(\psi_i)$	1
R_v	3 m	Ψ_C	$\pi/3$
L	2.15 m	$\Phi_{1/2}$	$\pi/3$
n	1.5	A_r	1 cm^2
ζ	2	$P_{\max}^{\mathrm{VLC}}$	9 W
η	0.5 A/W	$P_{\max}^{\mathrm{RF}}$	200 mW
K_r	2.41		

In this regard, in Fig. 3, $\beta = 0.5$ meaning that both networks are equally accountable for the energy consumption of the network, while the different values of α highlight whether priority is given to one user over the other in terms of achievable data rate. The optimal system configuration in terms of energy efficiency is then seen to be the cooperative hybrid mode over the pure VLC mode when the rate requirements of the users are low. However, when users require higher throughput, the RF link requires a very high amount of energy to comply, while VLC can achieve the constraints at a lower energy cost. Interestingly, for lower rates, as the rate threshold increases, energy efficiency is also increasing, which means that a little amount of additional power can provide a higher increase in data rate, which can be justified through (8), (9).

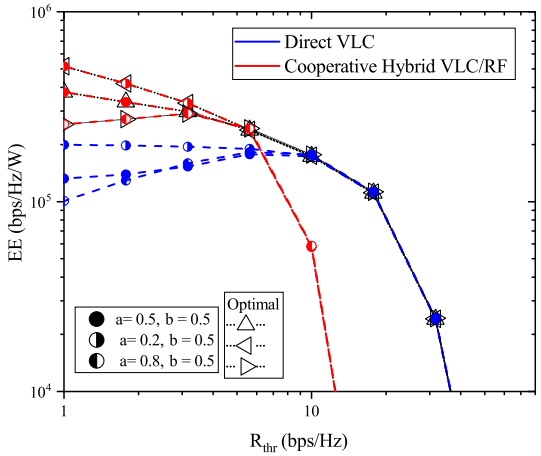

Fig. 3. Energy efficiency for different values of R_{thr} and α with $\beta = 0.5$.

Moreover, in Fig. 4, $\alpha = 0.5$ is set, so that neither U_1 nor U_2 has a higher priority than the other and the effect of different values of β are examined. When β is low, the power consumption of the VLC AP does not contribute a lot to the energy efficiency calculation. This is an interesting and practical case, since VLC APs can most of the time provide illumination coverage and are already on, so β can be lower than 0.5 or even zero. On the other hand, when illumination is not required, β can be higher than 0.5 to highlight the increased cost of the VLC AP in this scenario. It can be observed from Fig. 4, that when β takes lower values, the optimal selection is the VLC for a lower required threshold rate. When the weight β is increased, despite its lower energy efficiency is general, the cooperative hybrid VLC/RF mode is selected, instead, for up to 6 bits/Hz threshold rate.

Finally, the results of the implemented MLP are shown in Fig. 5. The dataset contained 10^4 cases, 7000 of which were used for training, 1500 for validation, and 1500 for testing. Stochastic Gradient Descent (SGD) was utilized to optimize the MLP, while the binary cross-entropy was used as a loss function. The proposed MLP has an accuracy of 95%. The average energy efficiency achieved through the use of the MLP is very tight to the optimal bound. As such, the DNN implementation can indeed help alleviate the computational

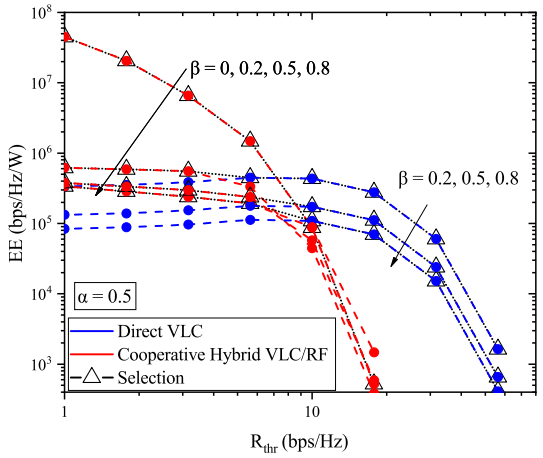

Fig. 4. Energy efficiency for different values of R_{thr} and β with $\alpha = 0.5$.

cost burden of the full optimization method described in section III.

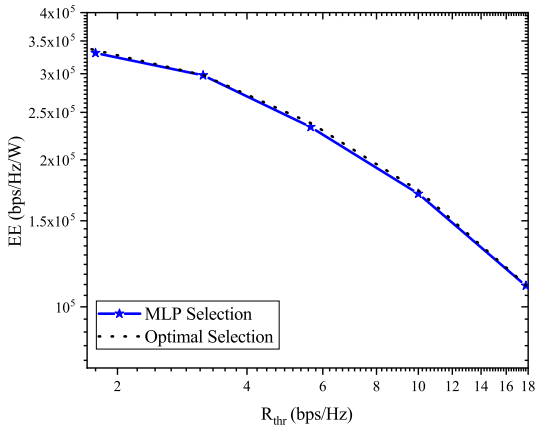

Fig. 5. Energy efficiency achieved through MLP selection and optimal selection for $\alpha = \beta = 0.5$.

VI. Conclusions

In this paper, we have presented a VLC network with NOMA that can operate in a cooperative hybrid VLC/RF mode to increase the energy efficiency of the system. A weighted energy efficiency metric was proposed to capture the particularities of the network and the optimal operation mode and power allocation was found via Dinkelbach's algorithm, DC programming and convex optimization methods. In order to reduce the computational complexity of the proposed solution a DNN was trained on optimal samples recorded from the optimal solution and reached an close to optimal performance. Future work of this project encompasses the training of the DNN to completely replace the optimization method after training and provide a close to optimal solution.

Acknowledgment

This publication is based upon work from COST Action CA19111 (European Network on Future Generation Optical Wireless Communication Technologies, NEWFOCUS), supported by COST (European Cooperation in Science and Technology).

References

[1] M. Uysal, C. Capsoni, Z. Ghassemlooy, A. Boucouvalas, and E. Udvary, *Optical Wireless Communications: An Emerging Technology*. Springer, 2016.

[2] M. Z. Chowdhury, M. K. Hasan, M. Shahjalal, M. T. Hossan, and Y. M. Jang, "Optical Wireless Hybrid Networks: Trends, Opportunities, Challenges, and Research Directions," *IEEE Commun. Surv. Tutor.*, vol. 22, no. 2, pp. 930–966, Jan. 2020.

[3] H. Marshoud, V. M. Kapinas, G. K. Karagiannidis, and S. Muhaidat, "Non-Orthogonal Multiple Access for Visible Light Communications," *IEEE Photon. Technol. Lett.*, vol. 28, no. 1, pp. 51–54, Jan. 2016.

[4] L. Yin, W. O. Popoola, X. Wu, and H. Haas, "Performance Evaluation of Non-Orthogonal Multiple Access in Visible Light Communication," *IEEE Trans. Commun.*, vol. 64, no. 12, pp. 5162–5175, Dec. 2016.

[5] Z. Yang, W. Xu, and Y. Li, "Fair Non-Orthogonal Multiple Access for Visible Light Communication Downlinks," *IEEE Trans. Wireless Commun. Lett.*, vol. 6, no. 1, pp. 66–69, Feb. 2017.

[6] B. Lin, W. Ye, X. Tang, and Z. Ghassemlooy, "Experimental demonstration of bidirectional NOMA-OFDMA visible light communications," *Opt. Express*, vol. 25, no. 4, pp. 4348–4355, Feb. 2017.

[7] V. K. Papanikolaou, P. D. Diamantoulakis, and G. K. Karagiannidis, "User Grouping for Hybrid VLC/RF Networks With NOMA: A Coalitional Game Approach," *IEEE Access*, vol. 7, pp. 103 299–103 309, Jul. 2019.

[8] Y. Xiao, P. D. Diamantoulakis, Z. Fang, Z. Ma, L. Hao, and G. K. Karagiannidis, "Hybrid Lightwave/RF Cooperative NOMA Networks," *IEEE Trans. Wireless Commun.*, vol. 19, no. 2, pp. 1154–1166, Feb. 2020.

[9] M. Obeed, H. Dahrouj, A. M. Salhab, S. A. Zummo, and M.-S. Alouini, "User Pairing, Link Selection, and Power Allocation for Cooperative NOMA Hybrid VLC/RF Systems," *IEEE Trans. Wireless Commun.*, vol. 20, no. 3, pp. 1785–1800, Mar. 2021.

[10] M. Obeed, H. Dahrouj, A. M. Salhab, A. Chaaban, S. A. Zummo, and M.-S. Alouini, "Power Allocation and Link Selection for Multicell Cooperative NOMA Hybrid VLC/RF Systems," *IEEE Commun. Lett.*, vol. 25, no. 2, pp. 560–564, Feb. 2021.

[11] M. Kafafy, Y. Fahmy, M. Abdallah, and M. Khairy, "Power Efficient Downlink Resource Allocation for Hybrid RF/VLC Wireless Networks," in *Proc. IEEE Wireless Communications and Networking Conference (WCNC)*. San Francisco, CA, USA: IEEE, Mar. 2017, pp. 1–6.

[12] A. Khreishah, S. Shao, A. Gharaibeh, M. Ayyash, H. Elgala, and N. Ansari, "A Hybrid RF-VLC System for Energy Efficient Wireless Access," *IEEE Trans. Green Commun. Netw.*, vol. 2, no. 4, pp. 932–944, Dec. 2018.

[13] S. Aboagye, A. Ibrahim, T. M. N. Ngatched, A. R. Ndjiongue, and O. A. Dobre, "Design of Energy Efficient Hybrid VLC/RF/PLC Communication System for Indoor Networks," *IEEE Wireless Commun. Lett.*, vol. 9, no. 2, pp. 143–147, Feb. 2020.

[14] J. Al-Khori, G. Nauryzbayev, M. M. Abdallah, and M. Hamdi, "Secrecy performance of decode-and-forward based hybrid rf/vlc relaying systems," *IEEE Access*, vol. 7, pp. 10 844–10 856, 2019.

[15] T. Komine and M. Nakagawa, "Fundamental Analysis for Visible-Light Communication System Using LED Lights," *IEEE Trans. Consum. Electron.*, vol. 50, no. 1, pp. 100–107, Feb. 2004.

[16] H. Ma, L. Lampe, and S. Hranilovic, "Coordinated Broadcasting for Multiuser Indoor Visible Light Communication Systems," *IEEE Trans. Commun.*, vol. 63, no. 9, pp. 3313–3324, Sep. 2015.

[17] A. Chaaban, Z. Rezki, and M. Alouini, "On the Capacity of the Intensity-Modulation Direct-Detection Optical Broadcast Channel," *IEEE Trans. Wireless Commun.*, vol. 15, no. 5, pp. 3114–3130, May 2016.

[18] W. Dinkelbach, "On Nonlinear Fractional Programming," *Management Science*, vol. 13, no. 7, pp. 492–498, Mar. 1967.

[19] N. Vucic, S. Shi, and M. Schubert, "DC programming approach for resource allocation in wireless networks," in *Proc. 8th International Symposium on Modeling and Optimization in Mobile, Ad Hoc, and Wireless Networks*. Avignon, France: IEEE, Oct. 2010, pp. 380–386.

[20] S. Boyd and L. Vandenberghe, *Convex optimization*. Cambridge university press, 2004.

[21] H. Sun, X. Chen, Q. Shi, M. Hong, X. Fu, and N. D. Sidiropoulos, "Learning to Optimize: Training Deep Neural Networks for Interference Management," *IEEE Trans. Signal Process*, vol. 66, no. 20, pp. 5438–5453, Oct. 2018.